

1 **A systematic analysis of metabolic pathways in the human gut microbiota**

2 Victòria Pascal Andreu<sup>1</sup>, Hannah E. Augustijn<sup>1,2#</sup>, Lianmin Chen<sup>2,3,#</sup>, Alexandra Zhernakova<sup>2</sup>, Jingyuan  
3 Fu<sup>2,3</sup>, Michael A. Fischbach<sup>4,5,7\*</sup>, Dylan Dodd<sup>5,6\*</sup>, Marnix H. Medema<sup>1\*</sup>

4 <sup>1</sup>Bioinformatics Group, Wageningen University, Wageningen, The Netherlands

5 <sup>2</sup>University of Groningen, University Medical Center Groningen, Department of Genetics, Groningen, Netherlands.

6 <sup>3</sup>University of Groningen, University Medical Center Groningen, Department of Pediatrics, Groningen, Netherlands

7 Department of Bioengineering<sup>4</sup>, Microbiology & Immunology<sup>5</sup> and Pathology<sup>6</sup>, Stanford University, Stanford, USA

8 <sup>7</sup>Chan Zuckerberg Biohub, San Francisco, CA USA

9

10 \* Correspondence: [ddodd2@stanford.edu](mailto:ddodd2@stanford.edu), [fischbach@fischbachgroup.org](mailto:fischbach@fischbachgroup.org), [marnix.medema@wur.nl](mailto:marnix.medema@wur.nl)

11 # Contributed equally

12

13 Keywords: specialized primary metabolism, metabolic gene clusters, gut microbiome, gutSMASH

14

15 **Abstract**

16 *The gut microbiota produce hundreds of small molecules, many of which modulate host physiology.*  
17 *Although efforts have been made to identify biosynthetic genes for secondary metabolites, the*  
18 *chemical output of the gut microbiome consists predominantly of primary metabolites. Here, we*  
19 *systematically profile primary metabolic genes from the gut microbiome, identifying 19,885 gene*  
20 *clusters in 4,240 high-quality microbial genomes. We find marked differences in pathway distribution*  
21 *among phyla, reflecting distinct strategies for energy capture. These data explain taxonomic*  
22 *differences in short-chain fatty acid production and suggest a characteristic metabolic niche for each*  
23 *taxon. Analysis of 1,135 subjects from a Dutch population-based cohort shows that the level of 14*  
24 *microbiome-derived metabolites in plasma is almost completely uncorrelated with the metagenomic*  
25 *abundance of the corresponding biosynthetic genes, revealing a crucial role for pathway-specific gene*  
26 *regulation and metabolite flux. This work is a starting point for understanding differences in how*  
27 *bacterial taxa contribute to the chemistry of the microbiome.*

28

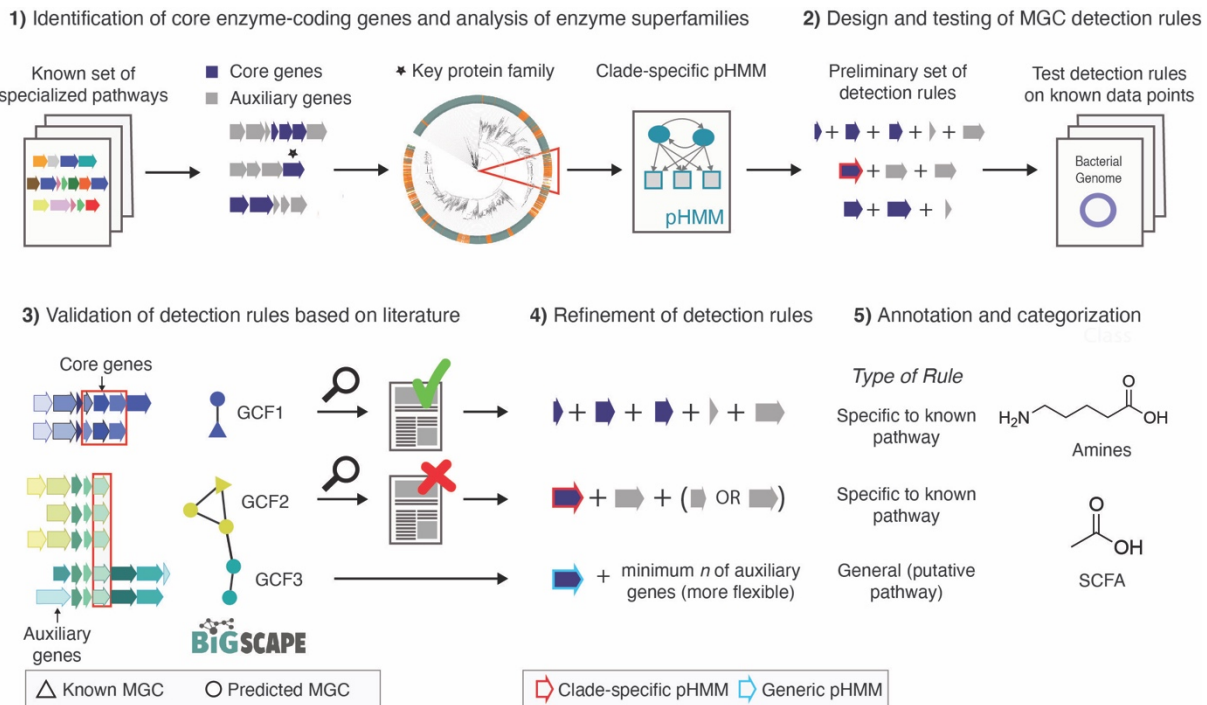
29 The pathways encoding the production of microbial metabolites are often physically clustered in the  
30 genome, in regions known as metabolic gene clusters (MGCs). Current tools for computational  
31 prediction of metabolic pathways focus on gene clusters for natural product biosynthesis (1) or generic  
32 primary metabolism (2, 3). Here, we introduce a new algorithm, gutSMASH, to profile known and  
33 predicted novel primary metabolic gene clusters from the gut microbiome. We use this tool to perform  
34 a systematic analysis of primary metabolic gene clusters in bacterial strains from the gut microbiome,  
35 and identify the prevalence and abundance of each of these pathways across a large population-based  
36 cohort.

37

38 Algorithms that identify physically clustered genes have become a mainstay of bacterial pathway  
39 identification; taking into account the conserved physical clustering of genes prevents false positive  
40 hits based on sequence similarity alone. This principle has been widely applied in the field of natural  
41 product biosynthesis, e.g. in antiSMASH (1), which predicts biosynthetic gene clusters (BGCs) by  
42 detecting physically clustered protein domains using profile hidden Markov Models (pHMMs). Here,

43 we tailored this gene cluster detection framework to detect MGCs involved in primary metabolism  
44 and bioenergetics.

45



46

47 **Figure 1: Development and design of detection rules for gutSMASH.** (1) A set of known and characterized MGC-encoded  
48 pathways were curated from the literature. Protein domains were identified across all MGCs and core enzymatic domains  
49 were manually identified. For enzymatic domains belonging to broad multifunctional enzyme families, protein superfamily  
50 phylogenies were built to create clade-specific pHMMs. (2) These domains were incorporated in the initial detection rules.  
51 The detection rules were run on a test set, and all the MGC predicted by the same rule were grouped together and (3) run  
52 through BiG-SCAPE, which grouped the MGCs into gene cluster families (GCFs). (4) Based on literature analysis of GCF  
53 members, detection rules were manually fine-tuned to either include or exclude MGC architectures that were either related  
54 to specialized primary metabolism or not. (5) Finally, fine-tuned detection rules were annotated and categorized into  
55 different MGC classes based on their metabolic end products.

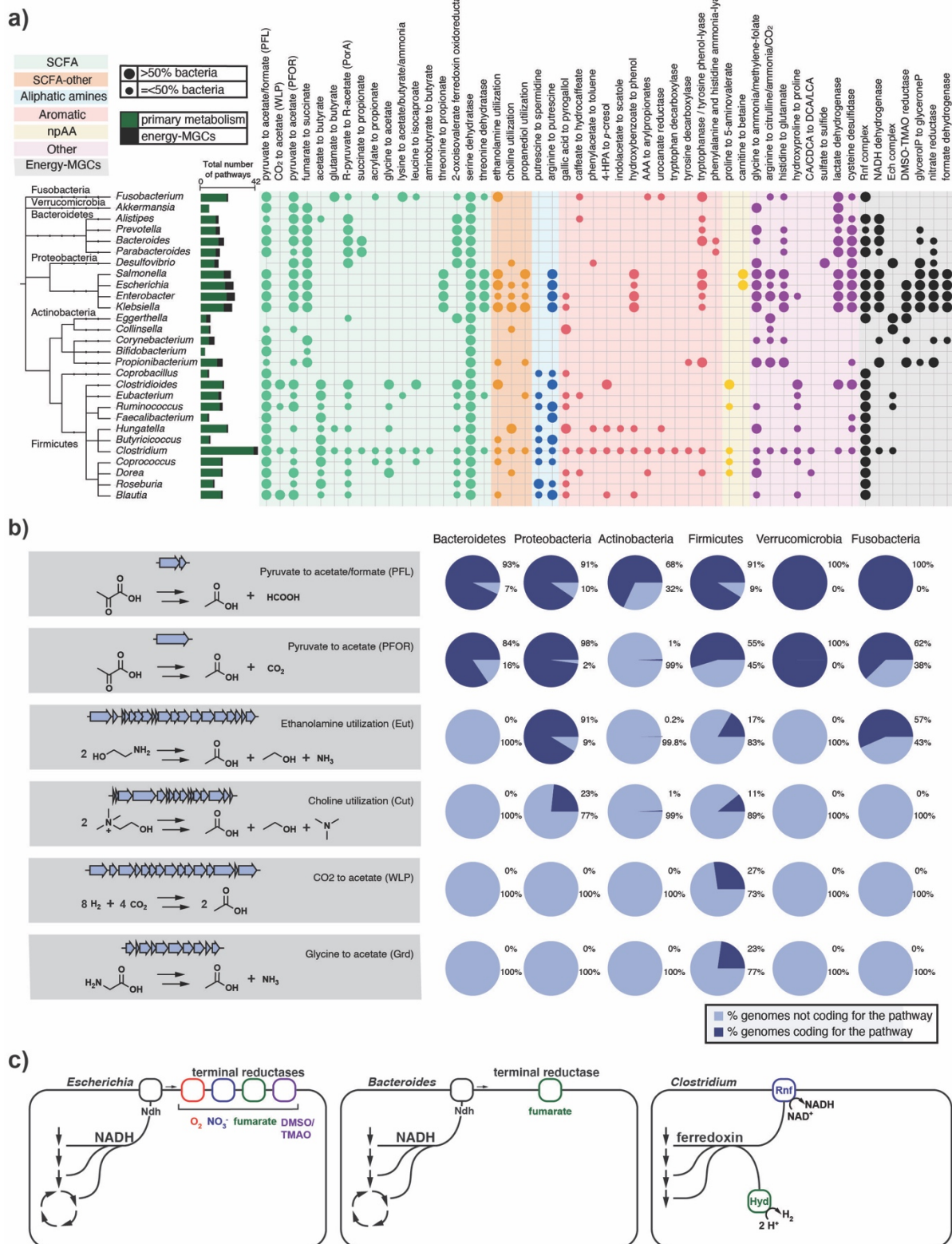
56

57 As a starting point, we constructed a dataset of 51 primary metabolic pathways from the gut  
58 microbiome with biochemical or genetic literature support (including MGCs as well as pathways  
59 encoded by a single gene) and identified core enzymes (i.e., required for pathway function) to serve  
60 as a signature for the detection rules (Figure 1, Table S1; see *Methods* for details). To more accurately  
61 predict MGCs of interest, we performed three computational procedures. First, for core enzymes  
62 belonging to 12 of the protein superfamilies that are known to catalyze diverse types of reactions and  
63 were most commonly found across a wide range of pathways, we constructed phylogenies and used  
64 them to create clade-specific pHMMs to detect specific subfamilies (see SI results *Phylogenetic*  
65 *analysis of protein superfamilies to identify pathway-specific clades*). Second, we designed pathway-  
66 specific rules for each MGC type in our dataset (see *Methods*). These rules were validated and  
67 optimized by detailed visual inspection and analysis of MGC sequence similarity networks made using  
68 BiG-SCAPE (4), generated from gutSMASH results on a set of 1,621 microbial genomes (Online Data:  
69 <https://gutsmash.bioinformatics.nl/help.html#Validation>); see SI results *Validation of gutSMASH*  
70 *detection rules by evaluating their predictive performance*) (Table S2&S3). Third, despite the fact that  
71 most specialized primary metabolic pathways are encoded in MGCs, there are also single-protein  
72 pathways that are in charge of the secretion of key specialized primary metabolites in the gut

73 microbial ecosystem, such as serine dehydratase, which produces ammonia and pyruvate from serine  
74 (5). For this reason, we also built 10 clade-specific pHMMs to detect these (see Methods section  
75 *Assessing single-protein pathway abundance within representative human gut bacteria*). The above  
76 procedures led to the design of a robust set of detection rules to identify both known and putative  
77 MGCs that are potentially relevant for metabolite-mediated microbiome-associated phenotypes.  
78

79 To profile the metabolic capacity of strains from the human gut microbiome, we selected a set of  
80 4,240 unique high-quality reference genomes consisting of 1,520 genomes from the Culturable  
81 Genome Reference (CGR) collection (6), 2,308 genomes from the Microbial Reference Genomes  
82 collection of the Human Microbiome Project (HMP) consortium (7) and 414 additional genomes from  
83 the class Clostridia to account for their metabolic versatility (8) (Table S4). We refrained from including  
84 metagenome-assembled genomes in this analysis, as they often lack the taxon-specific genomic  
85 islands (9) on which many specialistic metabolic functions are encoded. In total, gutSMASH predicted  
86 19,885 MGCs across these genomes that are clear homologues of MGCs for our set of known pathway  
87 types (See Methods: *Evaluating the functional potential of the human microbiome using gutSMASH*).  
88

89 The combined results of the gutSMASH MGC scanning and the single-protein pHMM detection across  
90 the three reference collections provide unique insights into the metabolic traits encoded by the  
91 genomes of human gut bacteria. While some genera harbor a small set of highly conserved pathways,  
92 (e.g., *Akkermansia*, *Faecalibacterium*), other genera contain much larger interspecies differences  
93 (Figure 2A). The genus *Clostridium* displays remarkable metabolic versatility, with 42 distinct  
94 metabolic pathways present across members of this genus (Figure 2A). Clostridial strains that are  
95 indistinguishable by 16S sequencing often harbor distinct gene cluster ensembles (Suppl. Figure 1),  
96 suggesting that specialization in primary metabolism leads to functional differentiation even among  
97 closely related strains. *Clostridium* is a clear outlier: by comparison, the next most numerous set of  
98 metabolic pathways are found within the Enterobacteriaceae (e.g., *Salmonella*, *Escherichia*,  
99 *Enterobacter*, and *Klebsiella*) with 22-25 metabolic pathways. Intriguingly, many of the metabolic  
100 pathways encoded by *Clostridium* and members of the Enterobacteriaceae are non-overlapping (with  
101 23/42 *Clostridium* pathways not being identified among Enterobacteriaceae), highlighting the distinct  
102 metabolic strategies these microbes employ within the gut (Figure 2A). The *Bacteroides*,  
103 Actinobacteria (*Eggerthella* and *Collinsella*) and Verrucomicrobia (*Akkermansia*) harbor a more  
104 restricted set of primary metabolic pathways, likely reflecting versatility in upstream components of  
105 their metabolism (i.e., glycan foraging and other forms of substrate utilization).  
106



107  
108 **Figure 2: Distribution of known pathways across most representative genera in the human gut.** (A) Circles represent the  
109 absence/presence of known pathways in each genus. Larger circles indicate cases in which more than 50% of the genomes  
110 for a genus encode the pathway, while smaller circles indicate cases in which 50% or fewer of the genomes encode it. Colored  
111 ranges indicate a categorization of MGCs by chemical class of their product, in which npAA represents nonproteinogenic  
112 amino acids and SCFA represents short-chain fatty acids. Taxonomic assignments were applied using the Genome Taxonomy  
113 Database (GTDB) (10). The tree was generated using phyloT (<https://phylot.biobyt.de/>) and visualized using iTOL (11). Raw  
114 data are available in Table S5. (B) Distribution of the main acetate synthesis pathways at phylum level. Some of the pathways  
115 are ubiquitous across the five major phyla (e.g. pyruvate to acetate/formate [PFL]), while others are only found in Firmicutes

116 (CO<sub>2</sub> to acetate [WLP]). Raw data for the pie charts is available in Table S6. Genes and gene clusters depicted are  
117 representatives from *Bacteroides thetaiotaomicron* (PFL & PFOR), *Salmonella enterica* (Eut), *Clostridium sporogenes* (Cut),  
118 *Clostridium difficile* (WLP) and *Clostridium sticklandii* (Grd). (C) Bioenergetic strategies in *Escherichia* that has a variety of  
119 alternate electron acceptors to choose from compared to *Bacteroides* and *Clostridium*. Abbreviations: PFL, pyruvate formate-  
120 lyase; PFOR, pyruvate:ferredoxin oxidoreductase; Eut, ethanolamine utilization; Cut, choline utilization; WLP, Wood-  
121 Ljungdahl Pathway; Grd, glycine reductase; CA, cholic acid; CDCA, chenodeoxycholic acid; DCA, deoxycholic acid; LCA,  
122 lithocholic acid; TMAO, trimethylamine N-oxide; DMSO, dimethylsulfoxide; SCFA, short-chain fatty acid; Ndh, NADH  
123 dehydrogenase, Rnf, Rhodobacter nitrogen fixation like complex; Hyd, hydrogenase.

124 Our results provide insights into the metabolic strategies that microbes use to produce short chain  
125 fatty acids (SCFAs). As expected, butyrate production is found exclusively in certain Firmicutes and  
126 Fusobacteria, whereas propionate production is largely confined to (and conserved in) the  
127 Bacteroidetes. However, the phylogenetic distribution of pathways that generate acetate -- the most  
128 concentrated molecule produced in the gut (12) -- has not yet been described. Two pathways for the  
129 conversion of pyruvate to acetate -- pyruvate formate-lyase (pyruvate to acetate/formate) and  
130 pyruvate:ferredoxin oxidoreductase (PFOR) -- are widely distributed across microbial strains from  
131 diverse phyla (Figure 2B). Two observations suggest that these two pathways are the most prolific  
132 source of acetate in the gut. First, some strains known to produce large quantities of acetate rely  
133 entirely on one or both of the pathways. Second, each one uses pyruvate as a substrate, consistent  
134 with a model in which these pathways are the primary conduit through which carbohydrate-derived  
135 carbon is converted to acetate. Additional taxon-specific pathways for acetate include the CO<sub>2</sub> to  
136 acetate pathway and the glycine to acetate pathway (each specific to a subset of Firmicutes), as well  
137 as the choline and ethanolamine utilization pathways (widespread among Enterobacteriaceae and  
138 each found in different clades of Firmicutes) (Figure 2A).

139  
140 Our results demonstrate a striking difference in mechanisms for energy capture by three of the major  
141 bacterial genera in the gut: *Bacteroides*, *Escherichia*, and *Clostridium*. When growing aerobically with  
142 glucose, *E. coli* generates most of its energy by channelling electrons through membrane bound  
143 cytochromes using oxygen as the terminal electron acceptor (Figure 2C). However, oxygen is limiting  
144 in the gut. Under anaerobic conditions, bacteria from the genus *Escherichia* employ alternate terminal  
145 electron acceptors such as nitrate, DMSO, TMAO, and fumarate by substituting alternate terminal  
146 reductases into their electron transport system (Figure 2C). However, in the healthy gut these  
147 alternate electron acceptors are either absent or available in limited amounts, likely explaining why  
148 these facultative anaerobes represent a small proportion of the healthy microbiome (13). In contrast  
149 to the diversity of terminal reductases used by the *Escherichia*, *Bacteroides* genomes encode only  
150 fumarate reductase (Figure 2C). They use a unique pathway, carboxylating PEP to form fumarate,  
151 which they use as a terminal electron acceptor to run an anaerobic electron transport chain involving  
152 NADH dehydrogenase and fumarate reductase, ultimately forming propionate. Thus, the metabolic  
153 strategy employed by *Bacteroides* ensures a steady stream of electron acceptor to fuel their  
154 metabolism. The *Clostridium* do not utilize similar mechanisms for energy capture as the *Escherichia*  
155 and the *Bacteroides*. Recent analyses suggest that they use the Rnf complex for generating a proton  
156 motive force. Several pathways encoded by the genomes of *Clostridium* (e.g., acetate to butyrate, AAA  
157 to arylpropionates, leucine to isocaproate) (Figure 2A) consist of an electron bifurcating acyl-CoA  
158 dehydrogenase enzyme. This complex bifurcates electrons from NADH to the low potential electron  
159 carrier ferredoxin which can then donate electrons to the RNF complex which functions as a proton  
160 or sodium pump, generating an ion motive force. Although much still is to be learned about Clostridial  
161 metabolism, our findings suggest that their metabolism operates at a different scale of the redox

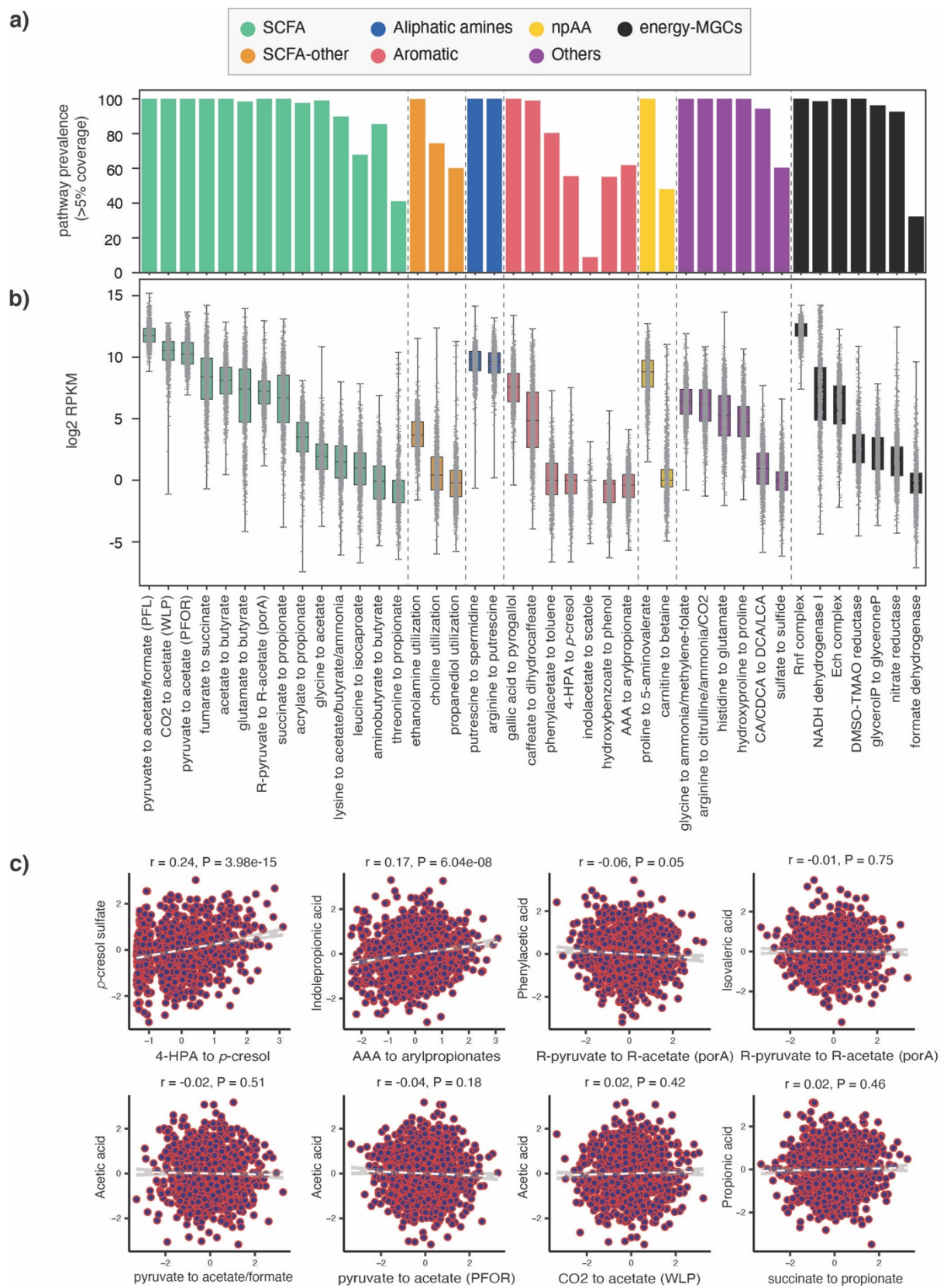
162 tower compared to *Bacteroides* and Enterobacteriaceae, using low potential electron carriers to fuel  
163 their metabolism.

164

165 Next, we set out to determine the prevalence and abundance of each pathway in a cohort of human  
166 samples. We used BiG-MAP (14) to profile the relative abundance of each MGC class across 1,135  
167 metagenomes from the population-based LifeLines DEEP cohort (15), by mapping metagenomic reads  
168 against a collection of 6,836 non-redundant MGCs detected in our set of reference genomes (Figure  
169 3A,B). Some pathways, such as CO<sub>2</sub> to acetate (acetogenesis) and butyrate production from acetate  
170 or glutamate, as well as polyamine-forming pathways, were found in >99% of microbiomes. Others,  
171 such as 1,2-propanediol utilization and *p*-cresol production, both associated with negative effects on  
172 gut health (16, 17), were observed at detectable levels in only half of the samples. In terms of  
173 abundance, it is striking that for example the bile acid-induced (*bai*) operon for the formation of the  
174 secondary bile acids deoxycholic acid and lithocholic acid, which has been characterized from very  
175 low-abundance *Clostridium scindens* strains (18), was still shown to be present in relatively high  
176 abundance across a subset of subjects. Analysis of the mapped reads showed that the vast majority  
177 of these mapped to a homologous MGC from the genus *Dorea* instead (Suppl. Figure 2), for which the  
178 physiological relevance remains to be established. It is also interesting to see that, while two of the  
179 three acetate-forming pathways (PFL and WLP) were consistently found at high abundance levels, the  
180 abundance of all butyrate-forming pathways is highly variable across subjects, with a >20-fold  
181 difference between lower and upper quartiles in the abundance distribution of the glutamate-to-  
182 butyrate pathway, and a >440-fold difference between the 10th percentile and the 90th percentile.

183

184 The wide variability in the metagenome abundance of each pathway raises the question of whether  
185 metagenomic abundance of a pathway correlates with the level of its small molecule product in the  
186 host. To address this question, we systematically compared the level of each pathway with the  
187 quantity of the corresponding metabolite as determined by plasma metabolomics. We find a striking  
188 lack of correlation between pathway and metabolite levels (*r* ranging from -0.04 to 0.24, Figure 3C).  
189 These data indicate that gene abundances in metagenomes are not (on their own) a useful predictor  
190 of metabolic outputs. This finding has important implications for analyses that make metabolic  
191 inferences from gene abundances (19) or the abundances of individual strains (20). We speculate that  
192 a more detailed understanding of the influence of diet, differences in gene regulation, characteristic  
193 pathway flux (turnovers per unit time per protein copy), and pharmacokinetic characteristics (e.g.,  
194 absorption, distribution, metabolism, and excretion) could ultimately enable the prediction of  
195 metabolite abundance from metagenome abundance. The systematic detection of the relevant genes  
196 and gene clusters by gutSMASH will provide a technological foundation for future studies in this  
197 direction, by allowing mapping of metatranscriptomic data to these accurately defined and  
198 categorized sets of genomic loci in order to understand which conditions and interactions are driving  
199 the expression of these pathways and the accumulation of their products.



200

201

202

203

204

205

**Figure 3. Prevalence and abundance of specialized primary metabolic pathways across 1,135 human microbiome samples.**

(A) Prevalence of each of the 41 known pathway classes across all microbiomes, measured as the percentage of samples in which core enzyme-coding genes of at least one reference MGC belonging to a given class were covered by metagenomic reads across >5% of their sequence length. This cutoff was kept low to avoid false negatives due to limited sequencing depth for low-abundance taxa (raw data available at Table S8). (B) Distributions of log2 RPKM relative abundance values of all 41

206 known pathway classes, categorized by product class, across all LifeLines DEEP metagenomes (raw data available at Table  
207 S9). (C) Limited correlation of genetic pathway abundance with abundance of metabolites in blood plasma.  
208  
209 The gutSMASH software constitutes, to our knowledge, the first comprehensive automated tool  
210 designed to identify niche-defining primary metabolic pathways from genome sequences or  
211 metagenomic contigs—even a full-fledged metabolic network reconstruction software like  
212 PathwayTools (21) (which uses the extensive MetaCyc database (22)) lacks detection capabilities for  
213 3 out of the 41 MGC-encoded pathways detected by gutSMASH (Table S7). Moreover, the  
214 identification of MGCs provides considerably increased confidence that detected homologues for a  
215 given pathway are truly working together. Downstream, detected MGCs can be used as input for read-  
216 based tools such as HUMAnN (23) or BiG-MAP (14) to measure abundance or expression levels of the  
217 encoded pathways. On top of these functionalities, the gutSMASH framework also facilitates  
218 identifying new (i.e., uncharacterized) pathways in the microbiome. To this end, we designed an  
219 additional set of rules to detect primary metabolic gene clusters of unknown function that harbor Fe-  
220 S flavoenzymes (24), glycyl-radical enzymes, 2-hydroxyglutaryl-CoA-dehydratase-related enzymes,  
221 and/or enzymes involved in oxidative decarboxylation. From this analysis of putative MGCs (see SI  
222 methods *Analysis of distant homologues and putative MGCs from CGR, HMP and Clostridioides*  
223 *dataset*), we found 12,259 putative MGCs from 760 different species, that, after redundancy filtering  
224 at 90% sequence similarity, were classified into 932 GCFs. Within these, we manually prioritized a  
225 range of gene clusters with unprecedented enzyme-coding gene content (see Suppl. Figure 4&5, SI  
226 Results *Analysis of putative clusters and distant homologues: relevant candidates to study further*).  
227 These can be a potential new source to discover new pathways and metabolites.

## 228 **Funding**

229 This work was supported by the Chan-Zuckerberg Biohub (M.A.F.), DARPA awards HR0011-15-C-0084  
230 and HR0112020030 (M.A.F.), NIH awards R01 DK101674, DP1 DK113598, and P01 HL147823; and the  
231 Leducq Foundation. A.Z. is supported by the ERC Starting Grant 715772, Netherlands Organization for  
232 Scientific Research NWO-VIDI grant 016.178.056, the Netherlands Heart Foundation CVON grant  
233 2018-27, and the NWO Gravitation grant ExposomeNL 024.004.017. J.F. is supported by the ERC  
234 Consolidator grant 10100167, the Netherlands Heart Foundation CVON grant 2018-27, and the  
235 Netherlands Organ-on-Chip Initiative, an NWO Gravitation project (024.003.001) funded by the  
236 Ministry of Education, Culture and Science of the government of the Netherlands. L.C. is supported by  
237 the Foundation de Cock-Hadders grant (20:20-13) and a joint fellowship from the University Medical  
238 Centre Groningen and China Scholarship Council (CSC201708320268). D.D. was supported by NIH  
239 award K08 DK110335.

## 240 **Conflict of interest**

241 MAF is a co-founder and director of Federation Bio, a co-founder of Revolution Medicines, and a  
242 member of the scientific advisory board of NGM Biopharmaceuticals. MHM is a co-founder of Design  
243 Pharmaceuticals and a member of the scientific advisory board of Hexagon Bio. DD is a co-founder of  
244 Federation Bio.

245

246 **References**

- 247 1. K. Blin, S. Shaw, K. Steinke, R. Villebro, N. Ziemert, S. Y. Lee, M. H. Medema, T. Weber, antiSMASH 5.0: updates to the secondary metabolite genome mining pipeline. *Nucleic Acids Res.* **47**, W81–W87 (2019).
- 250 2. P. D. Karp, R. Billington, R. Caspi, C. A. Fulcher, M. Latendresse, A. Kothari, I. M. Keseler, M. Krummenacker, P. E. Midford, Q. Ong, W. K. Ong, S. M. Paley, P. Subhraveti, The BioCyc collection of microbial genomes and metabolic pathways. *Brief. Bioinform.* **20**, 1085–1093 (2019).
- 254 3. S. Abubucker, N. Segata, J. Goll, A. M. Schubert, J. Izard, B. L. Cantarel, B. Rodriguez-Mueller, J. Zucker, M. Thiagarajan, B. Henrissat, O. White, S. T. Kelley, B. Methé, P. D. Schloss, D. Gevers, M. Mitreva, C. Huttenhower, Metabolic reconstruction for metagenomic data and its application to the human microbiome. *PLoS Comput. Biol.* **8**, e1002358 (2012).
- 258 4. J. C. Navarro-Muñoz, N. Selem-Mojica, M. W. Mullowney, S. Kautsar, J. H. Tryon, E. I. Parkinson, E. L. C. De Los Santos, M. Yeong, P. Cruz-Morales, S. Abubucker, A. Roeters, W. Lokhorst, A. Fernandez-Guerra, L. T. D. Cappelini, R. J. Thomson, W. W. Metcalf, N. L. Kelleher, F. Barona-Gomez, M. H. Medema, A computational framework for systematic exploration of biosynthetic diversity from large-scale genomic data. *Nat. Chem. Biol.* **16**, 60–68 (2020).
- 263 5. S. Kitamoto, C. J. Alteri, M. Rodrigues, H. Nagao-Kitamoto, K. Sugihara, S. D. Himpli, M. Bazzi, M. Miyoshi, T. Nishioka, A. Hayashi, T. L. Morhardt, P. Kuffa, H. Grasberger, M. El-Zaatari, S. Bishu, C. Ishii, A. Hirayama, K. A. Eaton, B. Dogan, K. W. Simpson, N. Inohara, H. L. T. Mobley, J. Y. Kao, S. Fukuda, N. Barnich, N. Kamada, Dietary L-serine confers a competitive fitness advantage to Enterobacteriaceae in the inflamed gut. *Nat. Microbiol.* **5**, 116–125 (2020).
- 268 6. Y. Zou, W. Xue, G. Luo, Z. Deng, P. Qin, R. Guo, H. Sun, Y. Xia, S. Liang, Y. Dai, D. Wan, R. Jiang, L. Su, Q. Feng, Z. Jie, T. Guo, Z. Xia, C. Liu, J. Yu, Y. Lin, S. Tang, G. Huo, X. Xu, Y. Hou, X. Liu, J. Wang, H. Yang, K. Kristiansen, J. Li, H. Jia, L. Xiao, 1,520 reference genomes from cultivated human gut bacteria enable functional microbiome analyses. *Nat. Biotechnol.* **37**, 179–185 (2019).
- 273 7. J. Lloyd-Price, A. Mahurkar, G. Rahnavard, J. Crabtree, J. Orvis, A. B. Hall, A. Brady, H. H. Creasy, C. McCracken, M. G. Giglio, D. McDonald, E. A. Franzosa, R. Knight, O. White, C. Huttenhower, Strains, functions and dynamics in the expanded Human Microbiome Project. *Nature* **550**, 61–66 (2017).
- 277 8. B. P. Tracy, S. W. Jones, A. G. Fast, D. C. Indurthi, E. T. Papoutsakis, Clostridia: the importance of their exceptional substrate and metabolite diversity for biofuel and biorefinery applications. *Curr. Opin. Biotechnol.* **23**, 364–381 (2012).
- 280 9. F. Maguire, B. Jia, K. L. Gray, W. Y. V. Lau, R. G. Beiko, F. S. L. Brinkman, Metagenome-assembled genome binning methods with short reads disproportionately fail for plasmids and genomic Islands. *Microb. Genom.* **6**, mgen.0.000436 (2020).
- 283 10. D. H. Parks, M. Chuvochina, D. W. Waite, C. Rinke, A. Skarszewski, P.-A. Chaumeil, P. Hugenholtz, A standardized bacterial taxonomy based on genome phylogeny substantially revises the tree of life. *Nat. Biotechnol.* **36**, 996–1004 (2018).
- 286 11. I. Letunic, P. Bork, Interactive Tree Of Life (iTOL) v4: recent updates and new developments. *Nucleic Acids Res.* **47**, W256–W259 (2019).

- 288 12. J. H. Cummings, E. W. Pomare, W. J. Branch, C. P. Naylor, G. T. Macfarlane, Short chain fatty  
289 acids in human large intestine, portal, hepatic and venous blood. *Gut* **28**, 1221–1227 (1987).
- 290 13. S. A. Jones, T. Gibson, R. C. Maltby, F. Z. Chowdhury, V. Stewart, P. S. Cohen, T. Conway,  
291 Anaerobic respiration of *Escherichia coli* in the mouse intestine. *Infect. Immun.* **79**, 4218–4226  
292 (2011).
- 293 14. V. P. Andreu, H. E. Augustijn, K. van den Berg, J. J. J. van der Hooft, M. A. Fischbach, M. H.  
294 Medema, BiG-MAP: an automated pipeline to profile metabolic gene cluster abundance and  
295 expression in microbiomes. *BioRxiv*, doi:10.1101/2020.12.14.422671 (2020).
- 296 15. E. F. Tigchelaar, A. Zhernakova, J. A. M. Dekens, G. Hermes, A. Baranska, Z. Mujagic, M. A.  
297 Swertz, A. M. Muñoz, P. Deelen, M. C. Cénit, L. Franke, S. Scholtens, R. P. Stolk, C. Wijmenga, E.  
298 J. M. Feskens, Cohort profile: LifeLines DEEP, a prospective, general population cohort study in  
299 the northern Netherlands: study design and baseline characteristics. *BMJ Open* **5**, e006772  
300 (2015).
- 301 16. F. Faber, P. Thiennimitr, L. Spiga, M. X. Byndloss, Y. Litvak, S. Lawhon, H. L. Andrews-Polymenis,  
302 S. E. Winter, A. J. Bäumler, Respiration of Microbiota-Derived 1,2-propanediol Drives  
303 *Salmonella* Expansion during Colitis. *PLoS Pathog.* **13**, e1006129 (2017).
- 304 17. M. Andriamihaja, A. Lan, M. Beaumont, M. Audebert, X. Wong, K. Yamada, Y. Yin, D. Tomé, C.  
305 Carrasco-Pozo, M. Gotteland, X. Kong, F. Blachier, The deleterious metabolic and genotoxic  
306 effects of the bacterial metabolite p-cresol on colonic epithelial cells. *Free Radic. Biol. Med.* **85**,  
307 219–227 (2015).
- 308 18. M. Funabashi, T. L. Grove, M. Wang, Y. Varma, M. E. McFadden, L. C. Brown, C. Guo, S.  
309 Higginbottom, S. C. Almo, M. A. Fischbach, A metabolic pathway for bile acid dehydroxylation  
310 by the gut microbiome. *Nature* **582**, 566–570 (2020).
- 311 19. H. Mallick, E. A. Franzosa, L. J. McIver, S. Banerjee, A. Sirota-Madi, A. D. Kostic, C. B. Clish, H.  
312 Vlamakis, R. J. Xavier, C. Huttenhower, Predictive metabolomic profiling of microbial  
313 communities using amplicon or metagenomic sequences. *Nat. Commun.* **10**, 3136 (2019).
- 314 20. G. M. Douglas, V. J. Maffei, J. R. Zaneveld, S. N. Yurgel, J. R. Brown, C. M. Taylor, C.  
315 Huttenhower, M. G. I. Langille, PICRUSt2 for prediction of metagenome functions. *Nat.*  
316 *Biotechnol.* **38**, 685–688 (2020).
- 317 21. P. D. Karp, P. E. Midford, R. Billington, A. Kothari, M. Krummenacker, M. Latendresse, W. K.  
318 Ong, P. Subhraveti, R. Caspi, C. Fulcher, I. M. Keseler, S. M. Paley, Pathway Tools version 23.0  
319 update: software for pathway/genome informatics and systems biology. *Brief. Bioinform.* **22**,  
320 109–126 (2021).
- 321 22. R. Caspi, R. Billington, I. M. Keseler, A. Kothari, M. Krummenacker, P. E. Midford, W. K. Ong, S.  
322 Paley, P. Subhraveti, P. D. Karp, The MetaCyc database of metabolic pathways and enzymes - a  
323 2019 update. *Nucleic Acids Res.* **48**, D445–D453 (2020).
- 324 23. E. A. Franzosa, L. J. McIver, G. Rahnavard, L. R. Thompson, M. Schirmer, G. Weingart, K. S.  
325 Lipson, R. Knight, J. G. Caporaso, N. Segata, C. Huttenhower, Species-level functional profiling of  
326 metagenomes and metatranscriptomes. *Nat. Methods.* **15**, 962–968 (2018).
- 327 24. V. Pascal Andreu, M. A. Fischbach, M. H. Medema, Computational genomic discovery of diverse  
328 gene clusters harbouring Fe-S flavoenzymes in anaerobic gut microbiota. *Microb. Genom.* **6**,  
329 mgen.0.000373 (2020).